International Journal of Civil Engineering (2024) 22:1565–1585
https://doi.org/10.1007/s40999-024-00970-5

RESEARCH PAPER

Influence of Slag, Silica Fume and Waste Tire Wire on High-Strength Characteristics of Geopolymer Concrete Cured Under Ambient and Oven Conditions

Ali İhsan Çelik[1]

Received: 1 December 2023 / Revised: 14 February 2024 / Accepted: 20 March 2024 / Published online: 25 April 2024
© The Author(s), under exclusive licence to the Iran University of Science and Technology 2024

Abstract

Higher strengths can be achieved using environmentally friendly geopolymer concrete (GPC). Granulated blast-furnace slag (GBFS) and silica fume (SF) were used together in high-strength GPC, and the GBFS + SF mixture was replaced with fly ash at total rates of 5, 10, and 15%. Recycled waste tire wires were added at rates of 1, 2, and 3% by weight. The samples were cured under ambient and oven conditions for 28 days and subsequently tested to characterize their compressive, flexural, and splitting tensile strengths. The test results indicated that adding waste tire wires significantly influenced the samples cured under ambient conditions, leading to a strength increment of up to 45 MPa—an improvement of approximately 50%. The oven-cured samples improved strength by approximately 21%, and the maximum compressive strength peaked at 65 MPa. This result can be used as a positive reference for high-strength concrete. The addition of 3% waste tire wire resulted in a flexural strength of 15 MPa in samples cured under ambient conditions and up to 23 MPa in those cured in an oven. The splitting tensile strength peaked at 16 MPa, which agrees with the bending strength. Scanning electron microscopy and energy-dispersive X-ray analysis were performed on these samples, and the results corroborated these findings, yielding robust supporting evidence for the obtained results.

Keywords Geopolymer concrete · High strength · Ambient curing · Oven curing · Waste tire wire · Granulated blast furnace slag (GBFS) · Silica fume (SF)

1 Introduction

Geopolymer concrete (GPC) is a variant of concrete manufactured using alkaline activators and fly ash (FA)-like binders instead of ordinary Portland concrete (OPC). OPC production results in high emissions of CO_2, which is an important marker of industrial activity. These emissions contribute to global warming and environmental problems [1–5]. This form of concrete is particularly favored for its ability to offer characteristics like enhanced strength, resistance to chemicals, and ecological sustainability. Compared to OPC, GPC production offers benefits such as diminished CO_2 emissions and ecological sustainability [6–8]. High-strength GPC also represents a subcategory with enhanced mechanical attributes. In the construction industry, particularly for projects requiring resilience and distinct specifications, a preference for high-strength GPC is evident. However, factors such as manufacturing process, cost, and application requirements must be considered. Typically, concrete components are allowed to cure naturally at room temperature after casting. However, when slag was incorporated into the initial materials to partially substitute FA, this addition prompted the geopolymer to undergo hardening at ordinary temperatures. This was attributed to the calcium content of the slag. Additionally, this modification leads to concrete achieving increased strength, both in its early stages and as it matures over time [9–11]. Geopolymer binders, which are materials activated by alkaline activators, have gained recognition as viable substitutes for OPC owing to their enhanced mechanical strength and durability [12–14]. The

✉ Ali İhsan Çelik
acelik@kayseri.edu.tr

[1] Department of Construction, Tomarza Mustafa Akincioglu Vocational School, Kayseri University, 38940 Kayseri, Turkey

geopolymerization process distinguishes itself from the hydration of traditional cement. Notably, the responsiveness of the binder components utilized in crafting GPC to silica plays a beneficial role in facilitating geopolymerization [15].

Recently, significant progress has been made in the development of FA-based GPC properties, and granulated blast furnace slag (GBFS) has emerged as a promising additive [16, 17]. Therefore, the combination of FA and GBFS-based GPC can be considered as an alternative to OPC when subjected to harsh environmental conditions [18]. The mechanism of ambient curing of GPC is similar to that of curing of OPC-based concrete. Generally, FA-based GPC curing involves chemical reactions and crystal formation. The inclusion of GBFS as a partial replacement for FA provides an overall improvement. This improvement was due to the simultaneous polymerization and hydration of the reaction mechanism from FA and GBFS, respectively [15]. Correct curing of the GPC ambient ensures that the material exhibits the desired strength, durability, and properties. Combining FA with GBFS significantly increases the compressive strength of GPC, and C–S–H/C–A–S–H gels are formed in the geopolymer matrix with a high CaO content in GBFS [19, 20].

Microsilica (MS) is a frequently used additive in the manufacturing of GPC. MS is typically derived from centrifugal FA produced during thermal energy generation. When incorporated into the production of GPC concrete by substitution with FA, which serves as a source of alumina and silica in specific proportions, the reaction process is expedited, facilitating the hardening and strengthening of GPC concrete. Duan et al., found that the addition had significantly improved the compressive strength of GPC [21]. In their investigation of the mechanical characteristics of ultrahigh-strength GPC, Tayeh et al. observed that the inclusion of more than 15% of the overall binder mass resulted in a notable enhancement in GPC's mechanical properties of GPC, particularly because of the significant contribution of MS additives [22]. Ekinci et al. reported that the highest compressive strength was achieved when the inclusion rates of MS (magnesia–silica) were set at 3 and 5% [23].

The incorporation of steel fiber reinforcement enhances the material flexibility and tensile strength by either postponing the emergence of cracks in concrete or impeding the spread of cracks when subjected to stress [24, 25]. Consequently, the deformation capacity and longevity of steel fiber concrete, which exhibits heightened tensile strength compared to conventional concrete, are likewise augmented [26–28]. This application may prove particularly advantageous for GPC, which is characterized by its brittle nature. Consequently, economical sizing of structural member sections becomes feasible when integrated with fiber-reinforced concrete reinforcements, particularly in scenarios where bending plays a significant role. The primary reason for concrete cracking is the presence of axial tensile stress. These tensile stresses can be effectively countered by strategically orienting steel fibers within the concrete [24]. The fibers act once the concrete has cracked, providing supplementary strength. Extensive studies have been conducted on this topic. Buratti et al. demonstrated that both steel and synthetic macrofibers significantly enhanced the response of concrete after cracking, yielding extra strength values that can be employed for design purposes [29]. Moreover, Bonakdar et al. reported that the introduction of steel fibers could transform the post-crack behavior of concrete from brittle to elastic under various loads, including compression, tension, bending, and impact [30]. Several studies have been conducted on the properties and performance of steel scrap concrete [31–35]. However, the literature on GPC is scarce. The addition of waste fibers at different rates has the potential to improve the mechanical properties of GPC, which has a brittle structure, such as compression and bending.

After determining that they have completed their useful life, original or coated tires that have been removed from vehicles cannot be used again as tires on the vehicle; this also includes tires that are rejected after production. Recycled waste steel wires can be extracted from discarded tires. Globally, approximately 1.5 billion tires are manufactured annually for automobiles and similar vehicles [36]. In Turkey, an average of 300,000 tons of end-of-life tires are produced annually from approximately 14 million vehicles. Currently, only 10% of the tires are processed through recycling, and their disposal at the end of their useful life poses a significant environmental challenge. The number of discarded tires is projected to peak at approximately 1.2 billion by 2030 as the number of vehicles continues to grow steadily. When stockpiled tires are considered, this figure is estimated to be approximately 5 billion [36–39]. Yıldızel et al. discovered that the inclusion of 2% waste wire sourced from automobile tire materials led to a notable decrease in crack formation and substantial enhancement in the strength characteristics of fabricated reinforced concrete beams [24]. Geopolymers are composite materials comprising two or more components. These components are skillfully combined to create a new material with the desired blend of characteristics [40, 41] In addition to the impressive mechanical properties of geopolymer concrete, they may exhibit undesirable fracture behavior, akin to other brittle materials, owing to their limited tensile and bending properties [21]. Thus, the incorporation of fibers into geopolymer matrices can lead to significant enhancements in the tensile strength and fracture energy. A recent study demonstrated that the addition of waste tire wires significantly improves the

fragile structure of GPC and increases its performance in terms of bending and compressive strength [4, 42].

High-strength concrete is a construction material that possesses elevated compressive and tensile strengths compared with standard concrete. This type of concrete is typically manufactured using distinct aggregates, cement variants, and chemical additives. High-strength concrete is favored in construction ventures, necessitating slender cross sections, extensive spans, or regions expected to bear heavy loads. Furthermore, they facilitate the creation of structures with reduced weight and slimmer profiles. Applications demanding formidable strength, such as bridges, tall edifices, aquatic installations, and industrial flooring, often extensively use high-strength concrete. According to ACI-363R [43], high-strength concrete is characterized by a compressive strength of 55 MPa or more. As outlined by Kamal Neupane et al., high-strength GPC is a specialized variant of concrete with a compressive strength exceeding 50 MPa [44]. Incorporating steel fibers into GPC results in a substantial improvement in the impact resistance and ductility, as documented in previous studies [45, 46]. Aydin and Baradan [47] demonstrated that the inclusion of 2% steel fibers measuring 6 and 13 mm in length had a minimal impact on the compressive strength, bending strength, and toughness. Furthermore, given the relatively high cost of these fibers, the precise control of their composition is imperative for commercialization and practical applications, as emphasized in the literature [48–50]. While some earlier investigations have indicated that incorporating MS into GPC leads to enhanced strength development, it concurrently diminishes workability, as documented in references [51–53]. In contrast, Wetzel and Middendorf revealed that the inclusion of adequate quantities of MS improves both the workability and compressive strength of GPC [54].

1.1 Research Significance

As compiled from the available literature, GBFS and SF have a remarkable effect on GPC production when the base binder is replaced with FA. Moreover, the incorporation of steel fibers appears to play a pivotal role in enhancing the mechanical properties of GPC. These collective endeavors have stimulated research on GPC as a cost-effective substitute for OPC. This study aims to investigate the strength of GPC and the impact of replacing FA with GBFS.

Typically, GPC is cured within a temperature range of 70–90 °C in an oven. However, shifting weather patterns and the quest for concrete alternatives to OPC have prompted researchers in the field of GPC to explore ambient curing conditions. The inclusion of GBFS plays a significant role in facilitating ambient curing of GPC [55]. In addition to GBFS, SF serves as a crucial filler and binder for ambient-cured GPC. In this study, GBFS + SF was used at levels of 5, 10, and 15%, with both ambient and oven curing. Additionally, the inclusion of waste tire fibers, an economical and ecologically significant recyclable material, at concentrations of 1, 2, and 3% is expected to substantially contribute to the GPC performance in terms of flexural strength, compressive strength, and tensile strength. When evaluating the effects of high-performance GPCs on flexural strength, it was revealed that the length of the steel fibers was a more important factor than their dosage or shape [47]. This result indicates that waste tire wires of different lengths and diameters will be more effective for the bending and compressive strength of GPC and will be more beneficial in terms of environmental impact. In this study, the samples cured under ambient conditions have the potential to be an alternative to OPC, whereas the samples cured in an oven will also serve as valuable references for cost-effective ready-mixed concrete production. In addition, if the compressive strength of the oven-cured samples exceeds 50 MPa, it serves as a reference for high-strength concrete.

2 Materials and Experimental Program

2.1 Materials

FA (Class F), which served as the primary binder in this study, was generously supplied through a grant from the Medcem Global Company. GBFS, a by-product employed in the iron manufacturing process, is typically acquired within blast furnaces operating at a temperature of 1500 °C. During this procedure, liquid iron is generated at the base of the furnace, whereas molten slag develops on the upper surface. The slag is then extracted from the furnace and rapidly cooled in water. Subsequently, it is transformed into a granular slag and ground, ultimately yielding the product, GBFS [17]. GBFS was also obtained under a grant from the Oyak Cement Company. Silica fume, often referred to as MS or condensed silica fume, is a finely powdered substance produced as a by-product during the manufacturing of silicon metal and ferrosilicon alloys. It primarily consists of silicon dioxide and trace amounts of elements, such as aluminum, calcium, and iron. When used alongside FA, silica fume contributes significantly to the pozzolanic reaction in GPC, thereby improving its mechanical properties [56, 57]. MS is readily available commercially. Some studies have indicated that GBFS has the potential to increase the fragility of GPC [58]. Other research efforts have been dedicated to mitigating the brittleness of GPC by adding polypropylene fibers [17]. Consequently, prior studies have provided a basis for investigating the incorporation of waste tire fibers

alongside GBFS in the production of GPC. Waste tire fibers, employed as steel fibers, were acquired through a grant from the Kudret construction company and sourced from the Viollas recycling facilities. Fine and coarse aggregates from Kayseri, Turkey, were generously provided by Eurostone. Sodium hydroxide (NaOH) and sodium silicate (Na_2SiO_3) are commercially available essential alkali activators. The main binding material for GPC is FA. However, some waste powders can increase the strength of GPCs and promote environmental sustainability. However, how these waste powders are used in GPC production and how the mixing ratios are adjusted may vary depending on the local requirements and specific conditions of the project. Based on previous studies, GBFS and FS were used in this study by substituting with FA in certain proportions. In addition, waste tire wires were added in various proportions. One of the samples obtained after mixing was cured in an ambient environment, and the other was cured in an oven. A flowchart of the study method is shown in Fig. 1.

Figure 2 displays samples of all the materials utilized in this experimental study. First, the aggregates and binders were mixed for approximately 1 min, and then the alkaline activators were slowly transferred into the mixer as if flowing from a tap. It was added by sprinkling while the mixture continued to ensure homogeneous distribution of the added wires without becoming tangled in the mixture. Fresh concrete was mixed in a mixer for approximately 5 min and filled into the molds.

Waste wires were randomly trimmed to a length of 20–70 mm. Additionally, the diameters of 100 wires were measured and noted individually with a micrometer. The frequency of their findings is plotted in Fig. 3. Steel fibers are widely used in high-strength GPC concrete to prevent brittle fracture, increase ductility and energy absorption, and improve mechanical performance [59]. Adding 1.5% by volume of steel fibers can increase the flexural fracture energy of ultrahigh-performance GPC by as much as 31 [60]. However, it has been stated that these small volumes will also affect the brittleness of high-strength GPC [61]. The size, shape, orientation, and quantity of fibers used in different bonding systems can directly affect their performance [62]. However, it has been reported that corrugated and twisted fiber shapes improve the known mechanical properties of conventional ultrahigh-performance OPC [62, 63]; however, using such fibers in ultrahigh-performance GPC leads to lower durability [15]. This can be attributed to the brittleness of the geopolymer binder with corrugated fibers, creating concentrated stress rather than an evenly distributed force in its microstructure [64]. When evaluating the effects of high-performance GPC on flexural strength, it has been reported that the length of the steel fibers is a more significant factor than their dosage or shape [47]. This change could offer an easier way to add various fiber types when producing composite materials without the need for special processing [64]. This finding suggests that incorporating waste tire wires with different lengths and diameters could be more effective in enhancing the bending and compressive strength of GPC, providing potential environmental benefits.

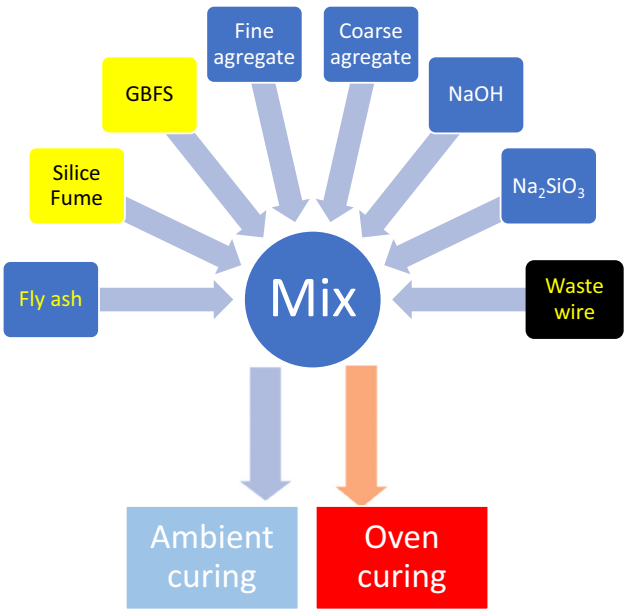


Fig. 1 Flowchart of the production method

To gather data on the stress–strain characteristics of the steel wires used for waste materials, three randomly selected wires were subjected to tensile testing at a speed of 10 mm/min in the ERUTAUM test laboratory at Erciyes University. As illustrated in Fig. 4, despite their high tensile strength, the selected wires do not exhibit ductile behavior. Furthermore, Wire 1 exhibited identical maximum yield elongation and rupture elongation of 0.97290 mm. Wire 2 exhibited a maximum yield elongation of 1.95057 mm and a rupture elongation of 1.07281 mm. Wire 3 exhibits a maximum yield elongation of 1.06120 mm and a rupture elongation of 0.50938 mm.

The tensile test results of the three waste wire samples focusing on the maximum stress, maximum force, maximum percentage elongation, and maximum elongation are presented in detail in Table 1.

The FA used in these experiments conformed to the ASTM C618-19 [65]. According to some studies, when low calcium FA is preferred for binder production, the CaO content should be less than 5%, the Fe_2O_3 content should be less than 10%, the LOI should be less than 5%, and the reactive silica content should be 40–50%. Additionally, the fineness of the FA should consist of particles in the range of 80–90%, and these particles should be smaller than

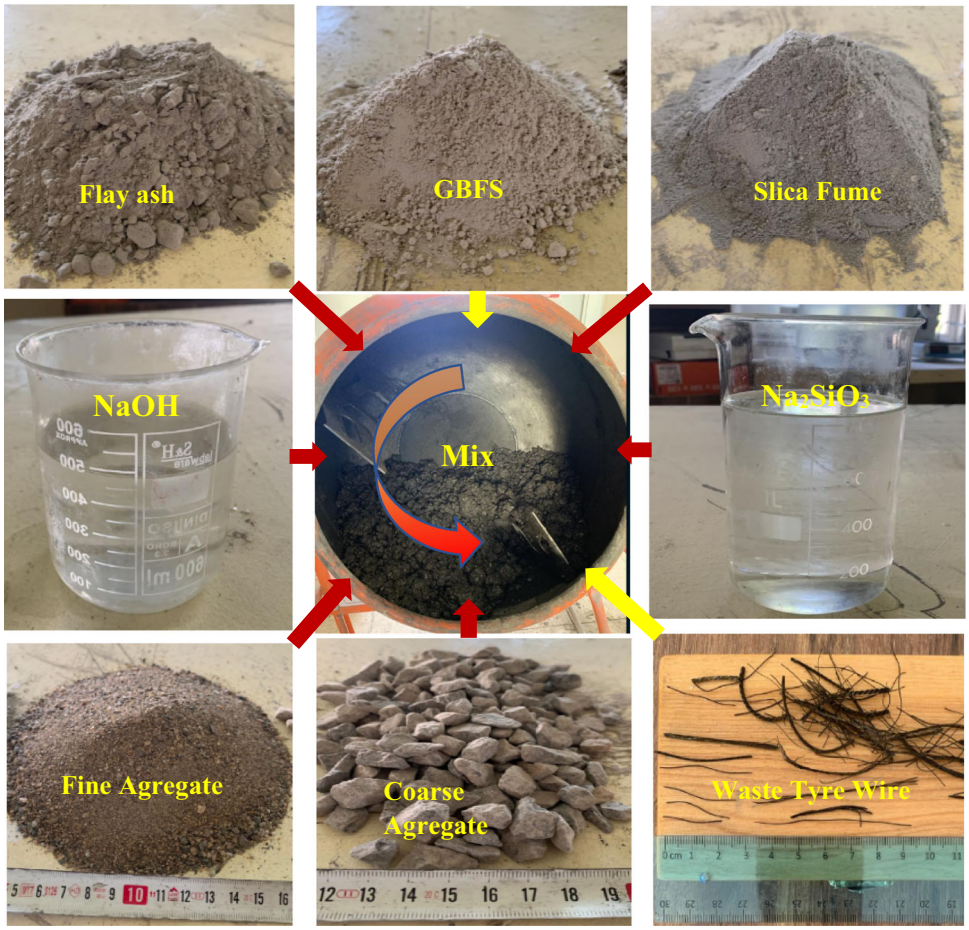


Fig. 2 Sample of materials

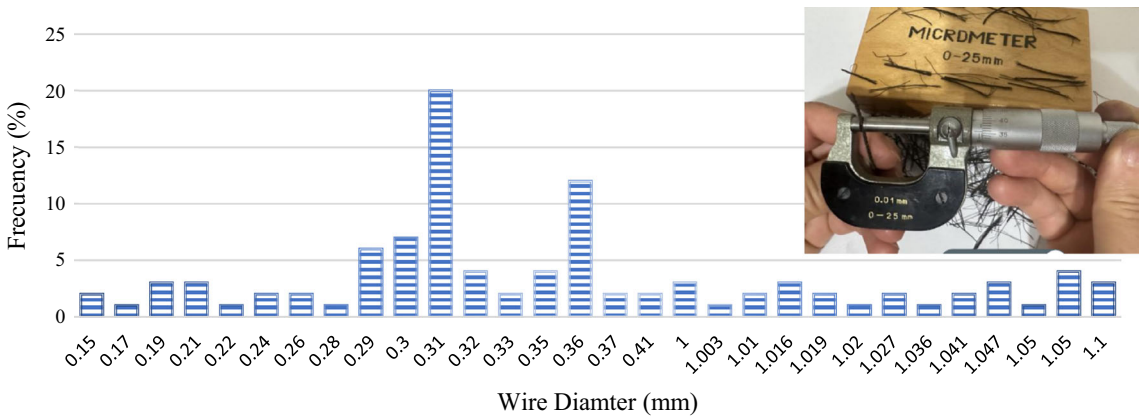


Fig. 3 Frequency of wire diameter

45 µm. Moreover, FA particles below 10 µm exhibit greater reactivity over 7 and 28 days, contributing to higher durability [66–68]. Table 2 presents the chemical compositions of the FA, GBSF, and SF components used in separate columns. The chemical compositions of the binder materials are listed in Table 2.

2.2 Experimental Program

In the context of the experimental study, 24 test setups were prepared and evenly divided into 12 for ambient curing conditions, and the remaining 12 were subjected to oven curing. The experiments designated AC were associated with ambient curing, whereas those labeled OC were

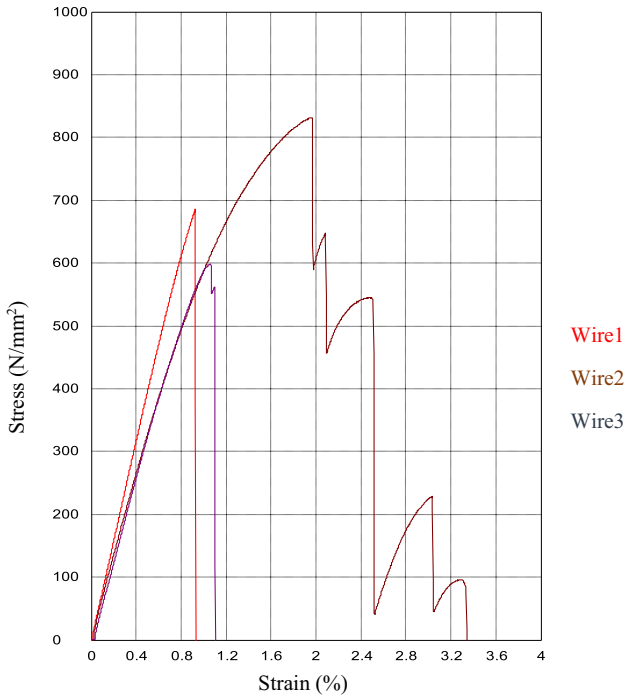


Fig. 4 Stress–strain test results of wires

associated with oven curing. In these experiments, various proportions of GBSF and SF were introduced as substitutes for a portion of the total FA content. Specifically, 3, 5, and 10% of the total FA were replaced with GBSF, whereas 2, 3, and 5% of the total FA were replaced with SF. This resulted in combinations in which the cumulative replacement of FA by GBSF and SF amounted to 5, 10, and 15%, respectively. Alkaline activator ratios were determined based on widely accepted values [68, 69]. These alkaline activators play a crucial role in facilitating geopolymerization within FA and other binding materials [70].

2.3 Casting Preparation and Sample Details

To cast GPC samples into cylindrical molds measuring 100 mm × 200 mm and prism molds measuring 40 mm × 40 mm × 160 mm, the following procedure was followed. Initially, GPC samples were mixed with FA, GBFS, and SF aggregates in a concrete mixer for approximately 2 min. Subsequently, the alkaline activator solutions were introduced into the mixer, and the mixing process was continued. The mixture was further mixed in the concrete mixer for approximately 8 min, and waste steel wires were gradually incorporated by sprinkling them into the mixture. Before transferring the fresh GPC mortar into the molds, a slump test was conducted to assess its consistency. During the filling process, fresh GPC mortar in the molds was skewed 25 times to ensure uniformity,

Table 1 Stress–strain result of wires

	Max stress (N/mm^2)	Max force (N)	Max percent elongation (%)	Max elongation (mm)	Area (mm^2)
Wire 1	685.862	538.675	0.92657	0.97290	0.785
Wire 2	831.219	652.838	1.95057	1.07281	0.785
Wire 3	598.284	469.891	1.06120	0.50938	0.785

	Max yield elongation (mm)	Ultimate_stress (N/mm^2)	Rupture force (N)	Perc. rupture elongation (%)
Wire 1	0.97290	685.862	538.675	0.92657
Wire 2	1.07281	542.600	426.157	2.50205
Wire 3	0.50938	557.435	437.808	1.08576

	Rupture elongation (mm)	Rupture deformation (mm)
Wire 1	0.97290	0.97290
Wire 2	1.37613	1.37613
Wire 3	0.52117	0.52117

Table 2 Chemical composition of binder materials

Component	Fly ash (%)	GBFS %	SF (%)
SiO_2	57.3	18.20	97
Al_2O_3	24.9	7.5	0.2
Fe_2O_3	6.05	0.1	0.5
CaO	3.98	67.60	0.2
SO_3	0.47	3.10	0.15
Na_2O	1.24	–	0.2
Cl^-	0.05	–	0.01
MnO	–	0.44	0.5
K_2O	–	0.76	0.5
TiO_2	0.7	0.95	0.02
NiO_3		0.04	–
SrO	–	0.019	–
ZrO_2	–	0.082	–
LOI (loss of ignition)	2.22	0.88	3.78
Sladge (> 45 μm)	17.4	0	



Fig. 5 Cylindrical and beam samples

followed by vibration on a shaking table for 20 s. Twelve samples were selected and kept in the laboratory for ambient curing for 28 days. The remaining 12 samples were stored in the laboratory for 48 h and then subjected to curing in an oven set at 85 °C for a 24-h duration. After oven curing, the samples were stored for an additional 28 days. The results and characteristics of the samples are observed in Fig. 5.

The standard quantities of Na_2SiO_3 145 kg/m^3 and NaOH were set at 58 kg/m^3 for all samples. The molarity of NaOH was prepared as 13 M for all the samples. Furthermore, the solution-to-binder ratio remained constant at 0.5, while the Na_2SiO_3/NaOH ratio was fixed at 2.5, and the NaOH molarity was prepared as 13 M. The fine aggregate had an average grain size of approximately 2 mm and a density of 145 kg/m^3. The coarse aggregate consists of crushed stone with particle sizes ranging from 7 to 11 mm, with an overall density of 1194 kg/m^3 [1]. The experimental design is summarized in Table 3. This refers to the ambient curing (AC) and oven curing (OC) in the sample code.

Table 3 Mixing amount of test samples (kg/m^3)

G no	Sample code	FA (kg/m^3)	GBFS (kg/m^3)	GBFS /FA	SF (kg/m^3)	SF// FA	Na_2SiO_3 (kg/m^3)	NaOH (13 M) (kg/m^3))	Fine aggregate (kg/m^3)	Coarse aggregate (kg/m^3)	Ratio of tire wire %	Ratio of GBFS + SF %
1st	AC1-05	385.70	12.18	0.3	8.12	0.2	145	58	643	1194	0	5
	AC2-10	365.4	28.42	0.7	12.18	0.3						10
	AC3-15	345.10	40.6	0.1	2.30	0.5						15
2nd	AC4-05	385.70	12.18	0.3	8.12	0.2	145	58	643	1194	1	5
	AC5-10	365.4	28.42	0.7	12.18	0.3						10
	AC6-15	345.10	40.6	0.1	2.30	0.5						15
3rd	AC7-05	385.70	12.18	0.3	8.12	0.2	145	58	643	1194	2	5
	AC8-10	365.4	28.42	0.7	12.18	0.3						10
	AC9-15	345.10	40.6	0.1	2.30	0.5						15
4th	AC10-05	385.70	12.18	0.3	8.12	0.2	145	58	643	1194	3	5
	AC11-10	365.4	28.42	0.7	12.18	0.3						10
	AC12-15	345.10	40.6	0.1	2.30	0.5						15
5th	OC1-05	385.70	12.18	0.3	8.12	0.2	145	58	643	1194	0	5
	OC2-10	365.4	28.42	0.7	12.18	0.3						10
	OC3-15	345.10	40.6	0.1	2.30	0.5						15
6th	OC4-05	385.70	12.18	0.3	8.12	0.2	145	58	643	1194	1	5
	OC5-10	365.4	28.42	0.7	12.18	0.3						10
	OC6-15	345.10	40.6	0.1	2.30	0.5						15
7th	OC7-05	385.70	12.18	0.3	8.12	0.2	145	58	643	1194	2	5
	OC8-10	365.4	28.42	0.7	12.18	0.3						10
	OC9-15	345.10	40.6	0.1	2.30	0.5						15
8th	OC10-05	385.70	12.18	0.3	8.12	0.2	145	58	643	1194	3	5
	OC11-10	365.4	28.42	0.7	12.18	0.3						10
	OC12-15	345.10	40.6	0.1	2.30	0.5						15



Fig. 6 Slump test

2.4 Slump Test

Slump testing is typically used to evaluate the workability, transportability, and quality of concrete. This test is an important tool widely applied in building material production and construction processes. In this study, a slump test was performed in accordance with the ASTM C143 standard to determine the critical performance properties of GPC concrete, such as the slump properties and homogeneity [71], as shown in Fig. 6.

2.5 Test Setup of Compression Strength

Prior to conducting the compressive strength tests, the samples underwent surface smoothing using a saw, as depicted in Fig. 7a. They were weighed for the unit volume density test, as shown in Fig. 7b. Compressive strength testing of the concrete was performed by applying a load to a sample at a constant rate, and when the sample broke, the applied maximum load value was recorded. The breaking point is usually where the sample breaks or begins to crack, and the compressive strength tests adhered to the ASTM C39/C39M (C39&C39M A, 2003) standard, as shown in Fig. 7c.

2.6 Setup of Flexural Strength Test

The flexural strength test of beams (dimensions: 40 mm × 40 mm × 160 mm) was performed at a single point at L/3 from the supports in the Kayseri University Construction Laboratory in accordance with the ASTM C 293 (ASTM-C293, 2015) standards [72]. A bending test schematic and an actual visual image are shown in Fig. 8a [2] and 8b.



Fig. 7 Praparation of the compressive test

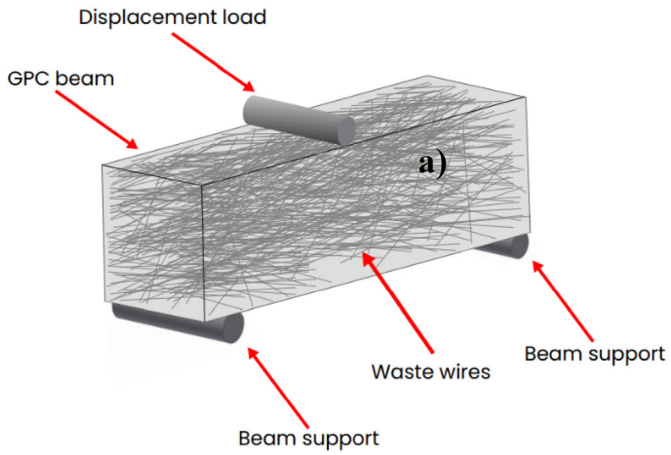




Fig. 8 Design of the flexural test



Fig. 9 Tensile strength testing setup

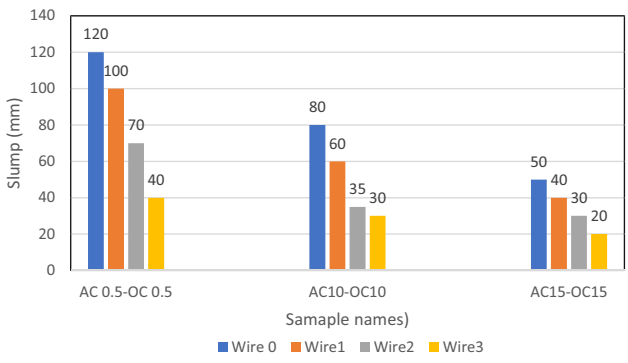


Fig. 10 Slump test results

2.7 Setup of Splitting Tensile Strength Test

Understanding the tensile strength of GPC is important when analyzing cracks and their structural aspects, particularly in applications demanding the use of high-strength concrete. In this study, which focused on high-strength GPC concrete subjected to both ambient and oven curing conditions, cylindrical samples were tested according to the ASTM C 476 standard [73], as depicted in Fig. 9.

3 Results and Discussion

3.1 Slump Value

In the context of GPC, it is crucial to ascertain the slump values and assess the workability. Figure 10 shows the slump test results for the sample castings subjected to both ambient and oven-curing conditions. FA was the main binder in GPC concrete. The most important component affecting the workability and setting time of fresh concrete

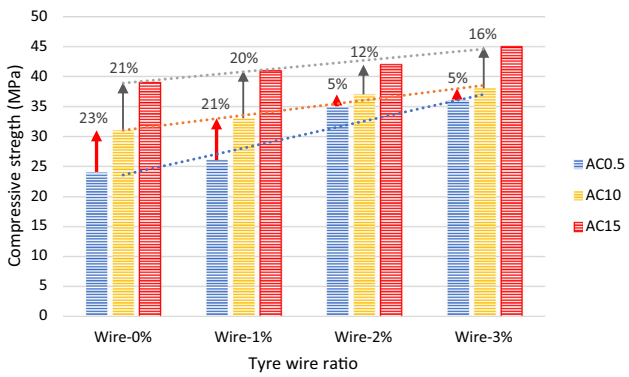


Fig. 11 Compressive strengths of samples cured under ambient conditions

was the calcium (Ca) ratio in the binder. When the Ca ratio in fly ash was 3.98, the ratio in the slag was determined to be 67.60. In this study, the slag ratio increases as the amount of fly ash decreases. With this increase, the slump values and setting time decreased as the Ca rate in the compound also increased. Typically, GPC exhibits slump values in the range of 100–150 mm. However, these values can fluctuate depending on factors such as the addition of binders, wires, and activator ratios. In particular, the slump values exhibited an inverse relationship with the increasing quantities of GBFS + SF and wire. As explained by Prusty and Pradhan, the reduced mobility of the FA particles can be attributed to the angular shape of the introduced GBFS particles [16]. In their research, they observed a comparable outcome. Shang et al. proposed that the alkaline activators employed in the mixture led to a decrease in the slump values because of their rapid gelation in conjunction with the inclusion of GBFS in the GPC [74]. In addition to the effect of the additional binders, it is evident that the added wires delay the slump. Similarly, in a recent study conducted by Çelik and Özkılıç with the addition of waste tire wire, they found that slump decreased with increasing wire ratio [2], indicating that the added wires provided integrity to the fresh concrete mortar and delayed its collapse.

3.2 Compressive Results of Ambient Curing Samples

Pressure tests were conducted after 28 days of exposure to ambient curing. The data presented in Fig. 11 demonstrate that substituting 5, 10, and 15% of the F-class FA, which is essentially GBFS + SF, resulted in compressive strengths of 25 MPa and higher. This result indicates that GPC can be effectively employed with ambient curing at specific substitution rates. When the waste wire ratio was 0% and the substitution rates were 5, 10, and 15%, compressive strengths of 24, 26, and 35 MPa were achieved. This outcome indicates the augmented formation of C–S–H gels, primarily attributable to the increased calcium content in GBFS, which fosters a denser matrix and augments the compressive strength. These findings agree with conclusions drawn by several researchers [16, 75, 76]. Figure 11 clearly illustrates that the inclusion of 1, 2, and 3% waste tire wires leads to a progressive increase in compressive strength. At a waste wire ratio of 3%, the compressive strength increased to 45 MPa, closely approaching the upper limit for high-strength concrete, which is typically 50 MPa. In a similar study in which ambient curing was performed with the addition of methacoline, a compressive strength of 36–56 MPa was obtained. Therefore, similar values were obtained in tests performed using different materials under ambient curing conditions [77]. These findings provide a promising reference point, suggesting that the desired 50 MPa benchmark might be attained by exploring various combinations of binders, activators, and waste wire ratios. However, owing to the diverse sizes and mechanical properties of recycled tire wires [2], a thorough investigation of GPC concrete incorporating waste wires, particularly under ambient curing conditions, is imperative.

Figure 12 presents the samples used in the compressive-strength tests. While it is observed that the samples that do not contain waste tire wire disintegrate after being broken, the fact that the samples containing the wire remain intact is an indication that they can stand without collapsing in the case of any structural damage.

3.3 Compressive Strength Results of Oven Curing Samples

Several studies have focused on oven-cured GPC, but studies on high-strength GPC are scarce [78–80]. This study highlights the environmentally friendly feature of high-strength GPC along with the addition of waste tire wires. As plotted in Fig. 13, in the first sample containing



Fig. 12 After the compressive test of samples

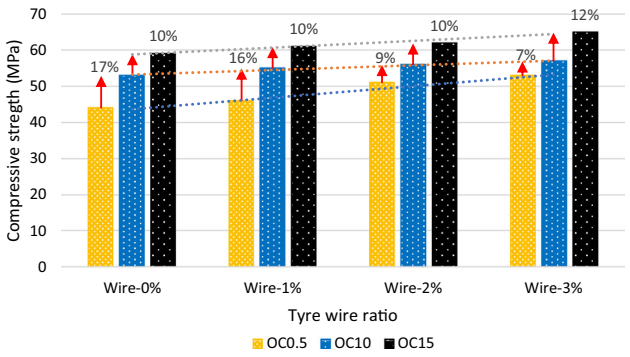


Fig. 13 Compressive strength of oven curing samples

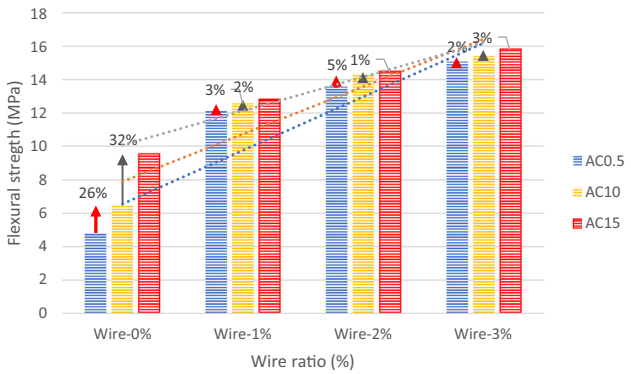


Fig. 14 Flexural strength of ambient curing samples

5% GBFS + SF without waste wire, the compressive strength was 44 MPa, whereas for GBFS + SF ratios of 10% and 15%, the compressive strength increased to 53 and 59 MPa, respectively. With the addition of 1% waste wire, the compressive strengths of 46, 55, and 61 MPa were obtained. With the addition of 2% wire, 51, 56, and 62 values were obtained, respectively, and all the values were in the high-strength concrete class. Finally, the addition of 3% wire yielded strengths of 53, 57, and 65 MPa. Although curing GPC in an oven at high temperatures initially causes pores to form, as the C-S-H gels grow, the voids are filled, and the strength increases [81]. The results confirmed those of similar studies [76].

3.4 Investigation of Flexural Strength After Ambient Curing

The flexural strength of GPC is affected by the materials used in the production, mixing ratios, and curing conditions. A slight increase in the flexural strength was observed with the progressive addition of GBFS + SF, as indicated by the slope lines in Fig. 14. Notably, the flexural strength improved further as the waste wire ratio increased. For instance, when the waste wire ratio was 0%, the flexural strengths were 4.83, 6.46, and 9.54 MPa. However, at a waste wire ratio of 1%, the flexural strengths notably were 12.13, 12.56, and 12.83 MPa. This represents an almost 50% difference between the two groups, underscoring the positive influence of wire addition on flexural performance. In the initial test, it is evident that the incorporation of the wire yields promising flexural performance. With a waste wire ratio of 2%, the bending strengths improved to 13.55, 14.28, and 14.49 MPa. Further increasing the wire content to 3% resulted in tensile strengths of 15.07, 15.401, and 15.82 MPa, respectively. Notably, the difference between the groups with wire addition was relatively minor, at approximately 8%. The chart displays the percentage change between the samples within the group, with the upward trend gradually diminishing. Similarly, the slope lines converge progressively as they approach the final column. This pattern illustrates that as the wire ratio increases, the flexural strengths become more closely aligned, indicating that further additions of wire are unlikely to significantly alter the flexural strength. This outcome could be attributed to the rigidity of the waste wire material. In addition, the tensile behavior of the wires exhibits a sharp transition from the yield point to the breaking point. Consequently, this characteristic led to more modest improvements in the flexural strength of the GPC with the incorporation of these wires. Similarly, Laxmi et al. achieved a flexural strength of 5.23 MPa in their study on GPC by incorporating hooked-end steel fibers and subjecting them to ambient curing with an 8 M NaOH solution [55]. In a recent study, the addition of 10%–60% GBFS and 1% glass fiber improved the flexural strength [82]. Although the obtained results overlap, increasing the mechanical performance of GPC cured under ambient conditions with lower GBFS rates and recycled waste tire wires is considered more important in terms of environmental impact; consequently, achieving a flexural strength of 15.83 MPa through the incorporation of 3% waste tire wire represents a significant advancement.

Figure 15 illustrates the deflection of the tested beam and the images of waste tire wires that effectively resist breakage (indicated using yellow markers). These findings indicate that the incorporation of wires restricts crack propagation. These outcomes align with research on GPC involving the addition of a hooked-end wire and ambient curing [55]. Furthermore, the results affirmed that the structures can withstand seismic events or similar stresses without collapsing.

3.5 Investigation of Flexural Strength After Oven Curing

The flexural strength of oven-cured GPCs has been extensively studied [1, 2, 20, 57, 68]. The brittle fracture of GPC has increased the importance of such studies. Previous studies have emphasized that oven-cured GPC has a brittle structure that often leads to a sudden collapse. In this experimental study, one of the biggest advantages of the added waste steel wires was their ability to reduce brittleness. In addition to the previous compression test results, it was determined that the brittleness decreased with an increase in the addition of steel wires in the tensile tests. This issue is particularly important for GPC, and similar studies should be conducted in the future to increase the ductility of oven-cured GPC using different fiber reinforcements. Figure 16 presents the results for 0% wire in the first group; an increasing amount of the GBFS + FS mixture provides a slight increase in flexural strength of



Fig. 15 Flexural strength damage

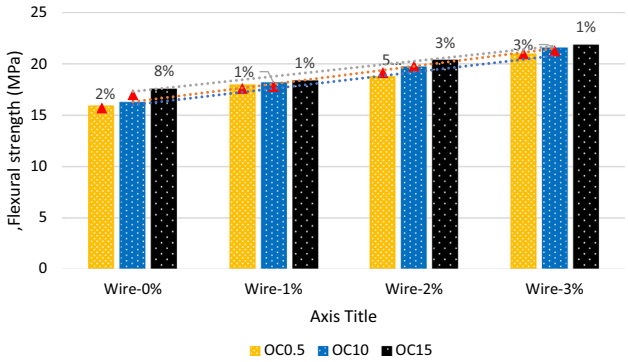


Fig. 16 Flexural strength of oven curing

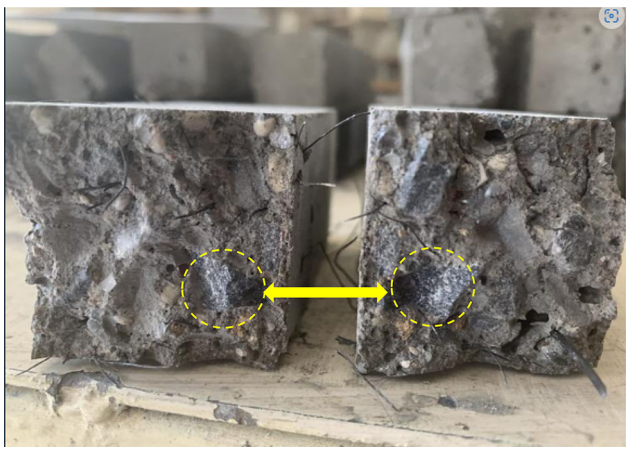


Fig. 17 Broken aggregate as a result of the flexural test

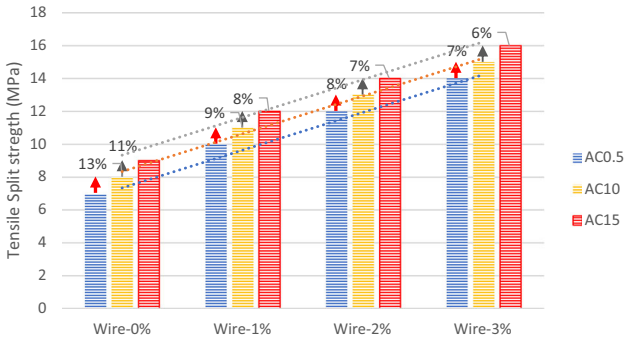


Fig. 18 Tensile split strength of ambient

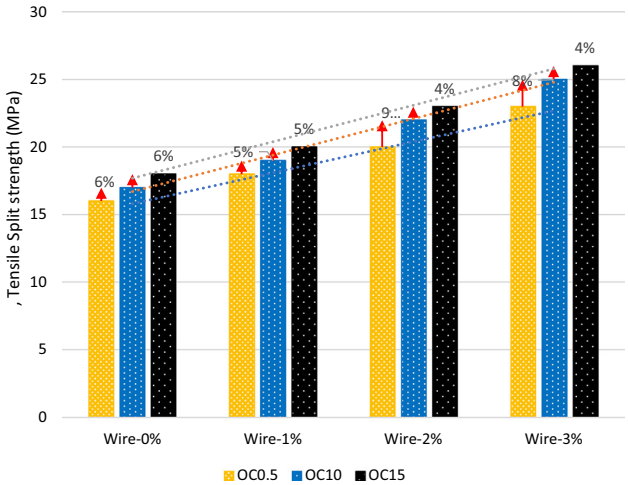


Fig. 19 Tensile split strength of the oven

15.86, 16.21, and 17.53 MPa. These results overlap with the ranges reported in previous studies [83]. The flexural strengths increase to 17.93, 18.14, and 18.33 MPa due to the addition of the 1% waste tire wire. Although the percentage increases within the group are shown in the graph, there is an increase of approximately 20% compared to the wireless group. When the wire ratio is 2%, the bending strengths are 18.73, 19.67, and 20.33 MPa, respectively. Finally, when the wire content is 3%, the bending strengths are 20.93, 21.51, and 21.80 MPa, respectively. The chart displays the percentage change between the samples within the group, with the upward trend gradually diminishing. Considering the eco-friendly feature of GPC, its performance is better compared to those reported in similar studies. In particular, our study achieved a higher level of results compared to those of a similar recent study [2].

Figure 17 presents the broken inner side of the sample containing 2% wire after the bending tests. The aggregate broke during bending and the binder and aggregates, together with the wire inside, yielded optimal bonding.

3.6 Tensile Split Strength Result of Ambient Curing

The splitting tensile test results for the GPC samples cured in the environment are plotted in Fig. 18. The obtained values are consecutive and almost identical. The increase in the samples within each group is shown as a percentage of the columns. These values surpass those reported in previous studies [55, 84], indicating the favorable impact of the addition of waste tire wire on the splitting tensile strength of GPC cured under ambient conditions. To quantify, the first group, not containing waste tire wire, registered strengths of 7, 8, and 9 MPa, samples containing 1% waste tire wire exhibited strengths of 10, 11, and 12 MPa, samples containing 2% waste tire wire exhibited strengths of 12, 13, and 14 MPa, and samples containing 3% wire yielded strengths of 14, 15, and 16 MPa.

3.7 Tensile Split Strength Result of Oven Curing

Figure 19 plots the splitting tensile test results of the oven-cured samples. In the samples that did not contain waste tire wires, the splitting tensile strengths were 16, 17, and 18 MPa. Samples containing 1% wire exhibited strengths of 18, 19, and 20 MPa, and samples containing 2% wire yielded strengths of 20, 21, and 22 MPa. Finally, samples containing 3% wire demonstrated strengths of 23, 25, and 26 MPa. The percentage changes between samples are depicted in the columns. Although the results were generally satisfactory, gradual and sequential increases were observed. The fact that the sloped lines are parallel to each other indicates a smooth increase. Recently, it was determined that there is an increase in the splitting tensile test results of GPC concrete produced with the addition of basalt fiber in the range of 3–18 [85]. These industrial materials do not consistently yield the anticipated results, and considering the production expenses, utilizing discarded rubber wires appears to offer greater advantages. In the future, segregating waste wires based on mechanical attributes such as tensile strength, yield strength, and breaking strength could potentially enhance the outcomes by utilizing wires with similar properties.

Because the sample depicted in Fig. 20a does not feature any wire content, it was dispersed while still in the press. The samples depicted in Fig. 20b and c did not separate even after exiting the press because they contained wires. In particular, GPC with waste tire wires can serve as an effective solution for reducing the formation of cracks in water tanks, nuclear power plants, airports, and road construction. A recent study demonstrated analogous findings, revealing that while certain fibers within the GPC fractured, others remained intact, preventing the complete separation of the structure [86]. This phenomenon has been previously attributed, in similar studies, to the variation in stress levels following cracking in samples containing steel fibers [2, 87–89].

4 Microstructure Analysis (SEM)

4.1 SEM Analysis of Samples Cured Under Ambient Conditions

Microstructure analysis (**SEM**) in concrete is an analysis performed to examine and evaluate the internal components and microstructures of concrete. It can also examine the size, shape, and distribution of cracks within concrete. This analysis also provides information about the durability, strength and other physical properties of concrete. In the experimental study, samples were taken from both ambient curing and oven curing and microstructure analysis was performed in Erciyes University TAUM laboratory. At the end of the analysis, it was tried to determine the distribution of components within the GPC samples,

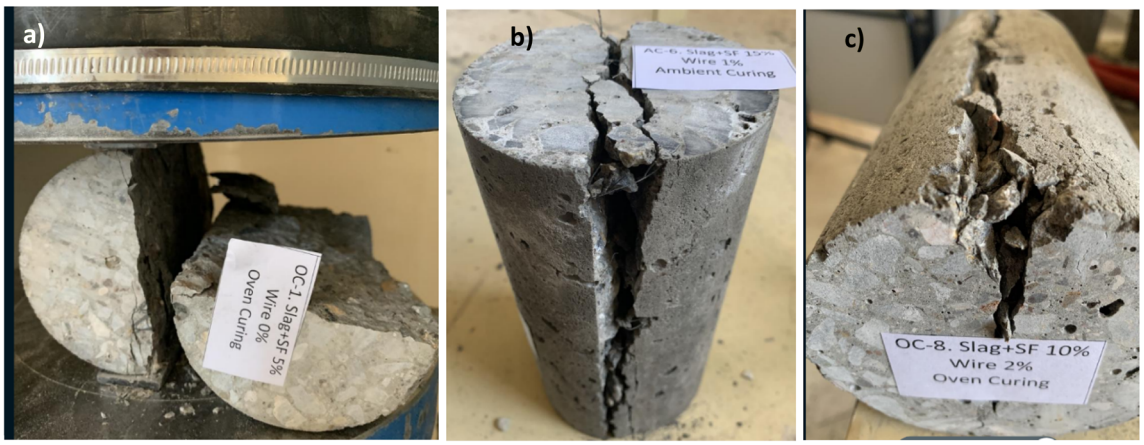


Fig. 20 Splitting of samples after tensile strength testing

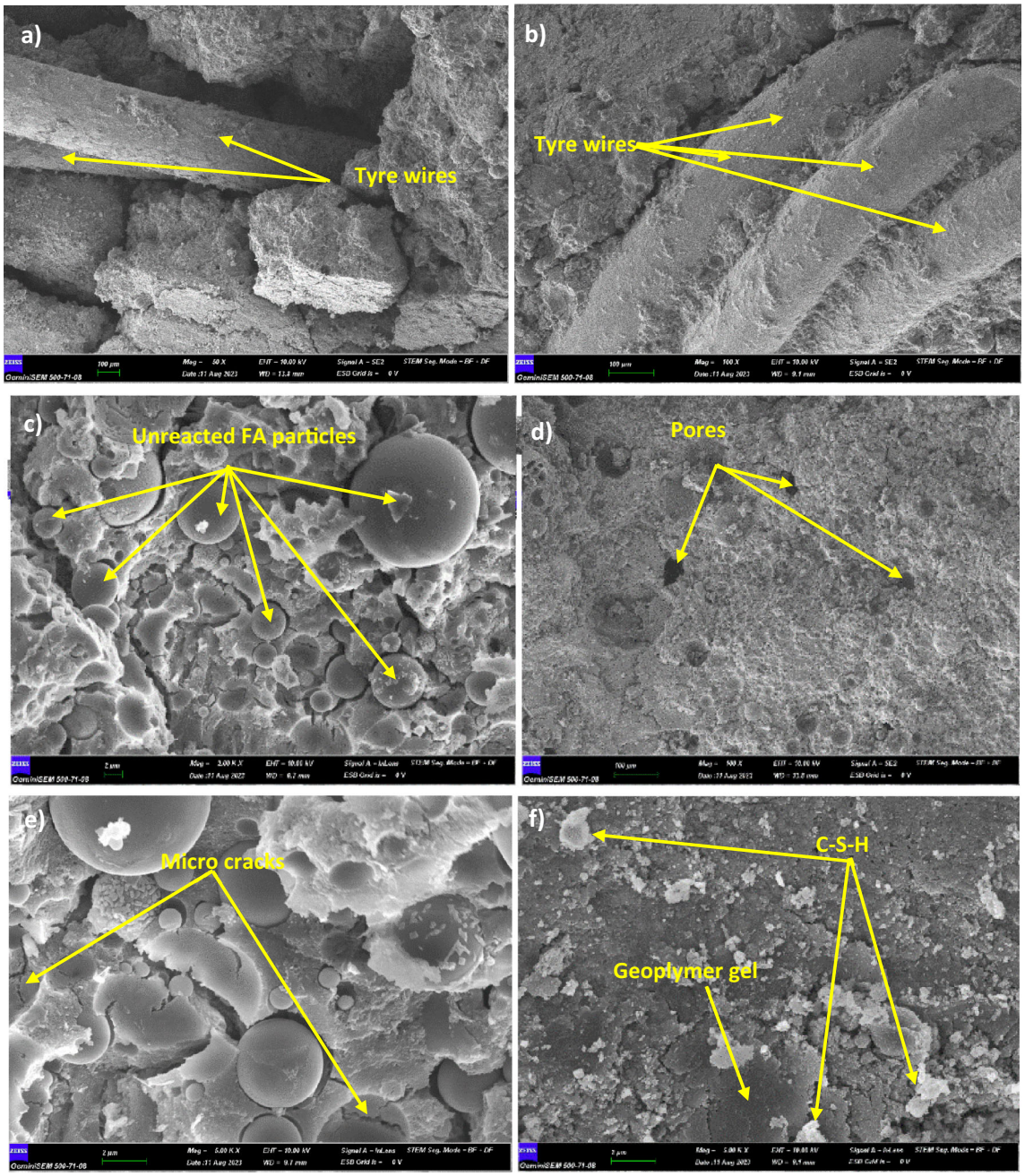


Fig. 21 SEM analysis results of ambient curing

porosity levels, distribution of aggregates, presence of cracks and other important microstructural features. Samples subjected to ambient curing exhibit a gradual increase in strength over time, potentially resulting in a higher porosity compared to samples cured in an oven [90]. This phenomenon can be attributed to the reduction of water content within the matrix during the oven curing process [91]. Figures 21a and b show the placement of waste wires in the GPC. It is seen that the wires provide integrity with the structure and bonding is achieved even between tight wires. This correlation's is evident from the results that they positively affect mechanical performance. In Fig. 21c, densely unreacted FA particles attract attention. A researcher discovered that with the addition of 10% more GBFS, the reaction in FA increased, and as the ratio increased, the number of unreacted FA particles decreased [92]. Figure 21d shows some pores, although not many. With the SF effect within the structure, the pores are reduced. In Fig. 20e, microcracks can be seen, albeit slightly, especially in the areas where unreacted FA

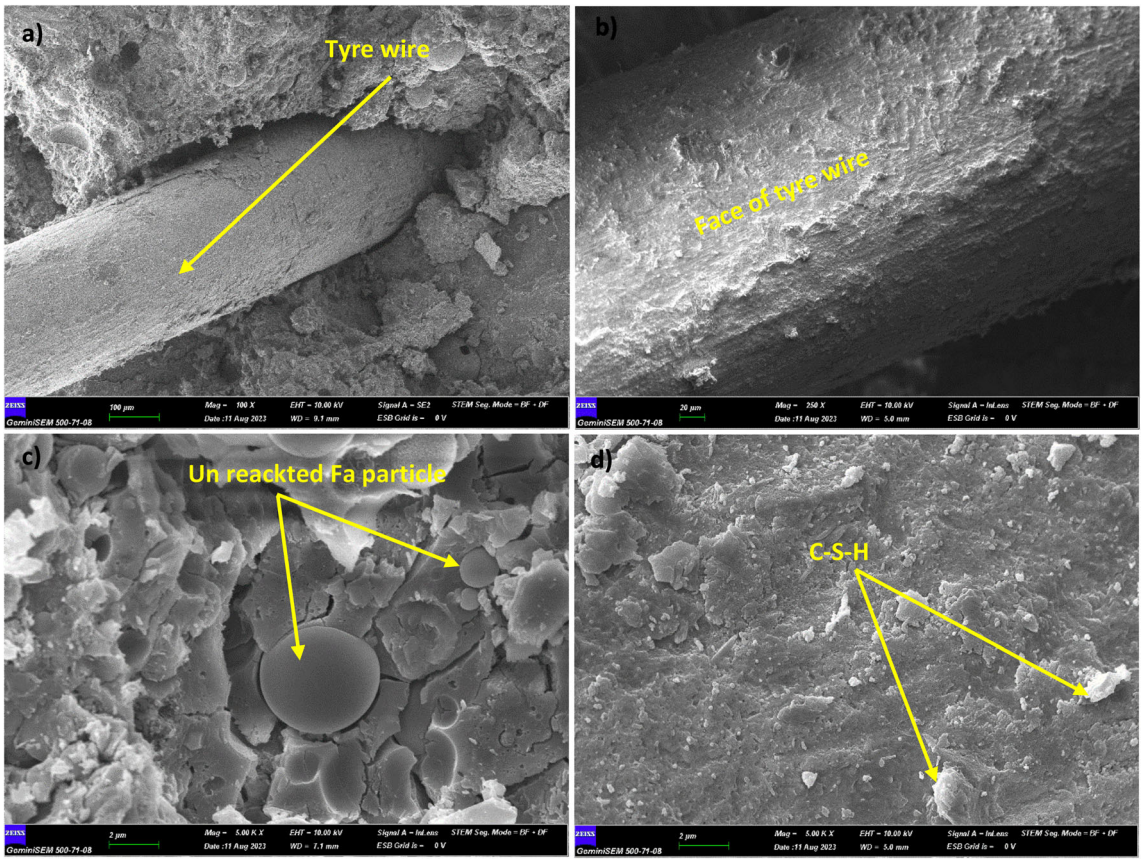


Fig. 22 SEM analysis results of oven curing

particles come into contact. In Fig. 21f, geopolymer gel formation and C–S–H formation are noteworthy. Low calcium in FA limits geopolymer gel formation [93], but the presence of GBFS increases geopolymer gel formation [93]. Geopolymer gel and C–S–H formation increase the strength in the structure.

4.2 SEM Analysis of Sample Oven Cured

Figure 22 shows the SEM analysis results of oven-cured samples. It is evident from the images that the GPC samples cured in the oven provide bonding and strength with a faster reaction. Figure 22a shows the position of the waste wire in the structure. A closer look at the wire in Fig. 22b shows that there is a good particle deposition on the surface. Figure 22c shows a small amount of unreacted FA particles. In Fig. 22d, intense C–S–H formation attracts attention. The results overlap with many studies conducted in the past [2, 94]. Excessive cracks and pores that negatively affect the mechanical properties of GPC are not seen in oven-cured samples. Curing temperature and curing time are effective here. Curing at 85 °C for 24 h results in a good reaction and bonding of the materials used, which also increases the inner surface quality.

5 EDX Analysis

5.1 EDX Analysis of Ambient Curing

EDX (energy-dispersion X-ray) analysis was performed to characterize the chemical compositions and structures of the samples obtained. In the sample scanned in Fig. 23a–c, the main elements are calcium (Ca), silicon (Si) and aluminum (Al). The weight atomic structure ratio of each element is given in detail in the table on the graph. The results coincide with similar studies [68]. Figure 23a shows the elements O, Na, Mg, Al, Si, K, Ca and Fe, respectively. Figure 23b focuses on a different point. Unlike Fig. 23a, K and Ca elements are not seen, while the presence of S, Cu, Zn and their elements attracts attention. In Fig. 23c, only O and S elements were found.

5.2 EDX Analysis of Oven Curing

Figure 24 shows the EDX analysis of GPC samples cured in the oven. The distribution of chemical elements within the structure is shown in the graph. The presence of high amounts of Ca, which is effective in providing high strength of GPC, attracts particular attention. In Fig. 24a,

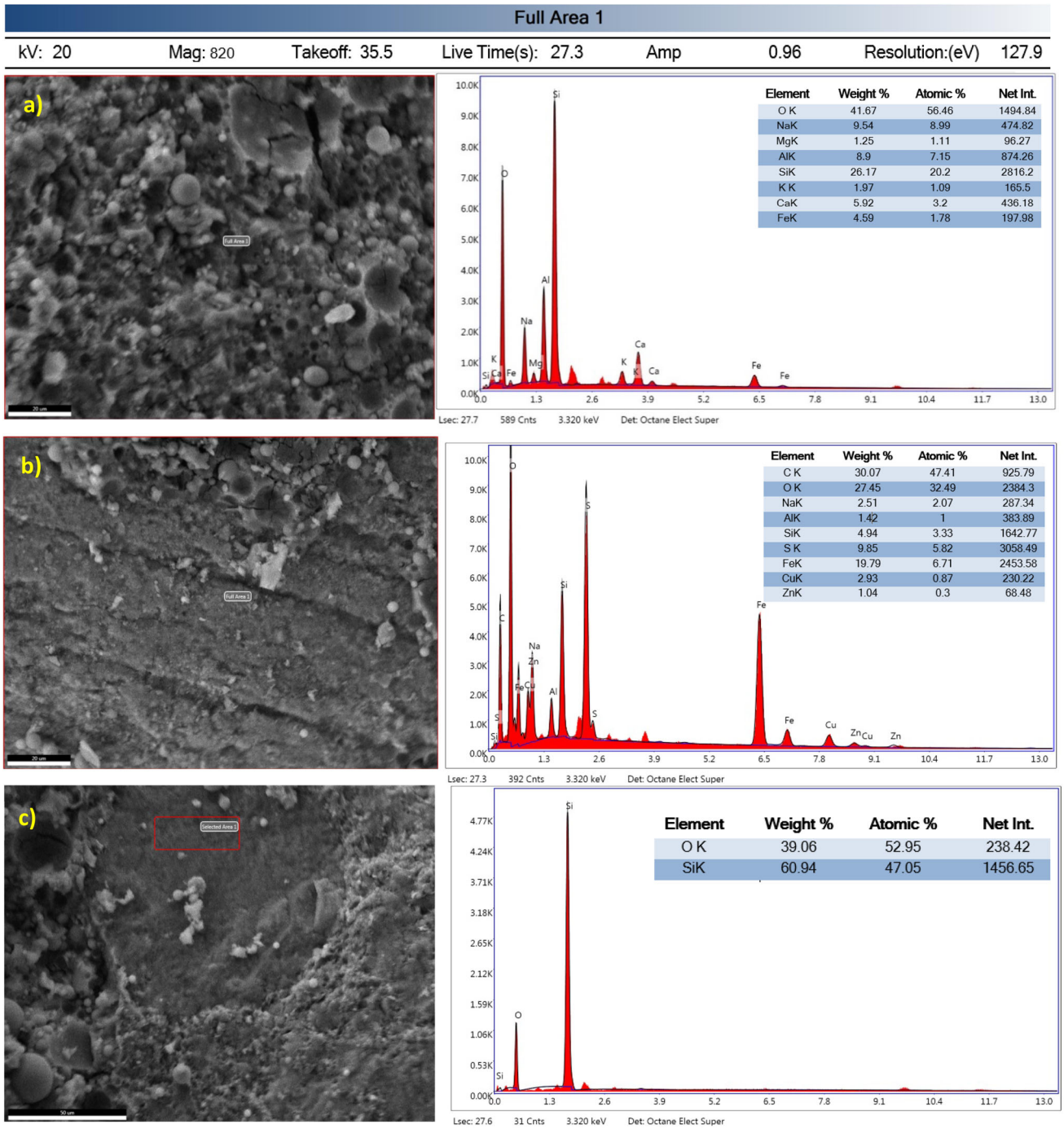


Fig. 23 EDX analysis result of ambient curing

the elements O, Na, Mg, Al, Si, K, Ca and Fe are present, respectively, and the presence of the same elements in Fig. 24b, based on the observation at a different point, shows that there is a homogeneous distribution. In Fig. 24c, the focus is on the aggregate surface and the presence of O, Na, Al, Si and K elements can be seen.

6 Conclusion and Recommendations

Interest in GPC is increasing, driven by environmental concerns and climate change. However, its practical application remains uncertain. One critical aspect is its structural usability and the possibility of preparation and curing, similar to that of OPC. Another significant challenge is the production of high-strength concrete using gel

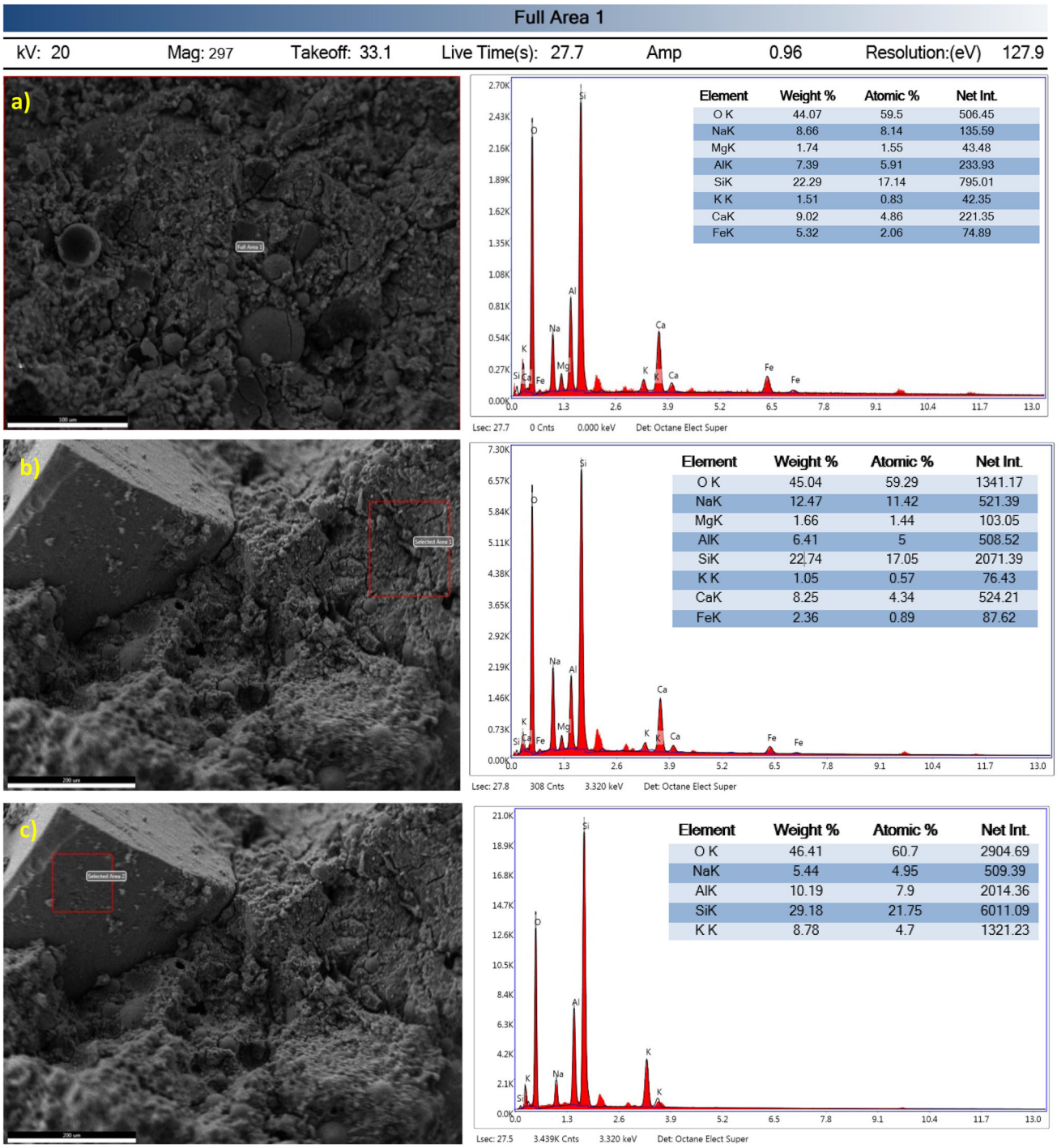


Fig. 24 SEM analysis results of oven curing

permeation chromatography. This research aimed to optimize the mechanical properties of GPC concrete, including compressive and flexural strength, through the incorporation of additional materials and improvements in curing conditions. Although FA serves as the primary binder material in GPC, its use alone does not always yield the required strength when cured under ambient conditions. To achieve the desired strength in GPC during ambient curing, additional materials are introduced, with GBFS being an important material. Owing to its substantial calcium content, GBFS has the potential to elevate GPC's strength to the desired level within 28 days of ambient curing, and it may continue to strengthen over time. In this study, blends of FA, GBFS, and FS were used in specific proportions. FA

was substituted with FA at percentages of 5, 10, and 15%. Furthermore, to rapidly achieve high-strength properties, recycled wires from waste tires, which pose environmental challenges, were incorporated into the mix at rates of 1, 2, and 3% by volume. The samples were classified into four groups. The first group received no wire addition, whereas the remaining three groups had wires added at specified rates. Some of these samples were left to cure in an ambient environment, while an equal number of samples underwent accelerated curing in an oven at 85 °C for 24 h. Following oven treatment, all samples were preserved for a total of 28 days, along with the samples cured under ambient conditions.

The main findings of this study are summarized as follows:

Slump test results The use of GBFS and ferrosilicate (FS) as binders reduced the slump values. This phenomenon is attributed to the high calcium content of GBFS. Furthermore, as the number of waste tire wires increased, the slump decreased. Specifically, when GBFS + FS was 5% and the waste tire wire ratio was 3%, the slump decreased by up to 20 mm.

Compressive strength achieved under ambient curing conditions The compressive strength of the samples cured under ambient conditions reached 45 MPa. Additionally, an increased GBFS + FS content led to an increase in the compressive strength by up to 21%. When 1% waste tire wire was added, the compressive strength increased by 21%. As the wire ratio increased, the rate of increase in compressive strength slowed. When the GBFS + FS ratio increased from 5 to 10%, there was a 23% increase in compressive strength. Similarly, when the ratio increased from 10 to 15%, the compressive strength increased by 21%. The addition of waste further augmented the compressive strength, albeit with a slight reduction in the rate of increase as the GBFS + FS ratio rose. The samples cured under ambient conditions have the potential to reach a compressive strength of 50 MPa in the future with more GBFS + FS additions and higher waste tire wire ratios.

Compressive strength achieved after curing in the oven GPC samples cured in the oven without wires achieved compressive strengths of 44, 53 and 59 MPa, whereas the addition of wires increased the compressive strength to 65 MPa. When the GBFS + FS ratio was 15%, the rate of increase in the compressive strength ranged from 10 to 12%. While the compressive strength in the initial sample was 44 MPa for the sample containing 5% GBFS + SF, these rates increased to 53 and 59 MPa for 10% and 15% GBFS + SF, respectively. With the addition of 1% waste wire, compressive strengths of 46, 55 and 61 MPa were obtained, respectively. With the addition of 2% wire, values of 51, 56 and 62 were obtained and all values fell into the high-strength concrete class. Finally, the addition of 3% wire provided strengths of 53, 57, and 65 MPa. Curing GPC in an oven with the addition of waste tire wires appears to be an effective method for producing high-strength concrete.

Flexural strength achieved under ambient curing conditions The samples cured under ambient conditions exhibited a significant increase in flexural strength. As the proportion of waste wire increased, there was a further improvement in flexural strength. For instance, at a waste wire ratio of 0%, the flexural strengths were 4.83, 6.46, and 9.54 MPa. However, with a 1% waste wire ratio, the flexural strengths increased to 12.13, 12.56, and 12.83 MPa, representing an almost 50% difference between the two groups and underscoring the positive impact of wire addition on bending performance. When the waste wire proportion reached 2%, the flexural strengths rose to 13.55, 14.28, and 14.49 MPa. When the waste tire wire addition was 3%, the final sample achieved a flexural strength of up to 15 MPa, which is considered high according to the literature standards. The oven-cured samples also exhibited improved flexural strength.

Flexural strength achieved after curing in the oven The flexural strengths of the samples cured in the oven have shown significant increases. The flexural strengths increase to 17.93, 18.14, and 18.33 MPa due to the addition of the 1% waste tire wire. Although the percentage increases within the group are shown in the graph, there is an increase of approximately 20% compared to the wireless group. When the wire ratio is 2%, the bending strengths are 18.73, 19.67, and 20.33 MPa, respectively. Finally, when the wire content is 3%, the bending strengths are 20.93, 21.51, and 21.80 MPa, respectively. The samples cured in the oven showed better results in terms of flexural strength.

Splitting tensile strength Splitting tensile strength of the samples cured under ambient conditions increased by an average of approximately 8% with increasing GBFS + FS and wire ratios. When the wire ratio reaches 3%, the splitting tensile strength increases to 16 Mpa.

SEM and EDX analyses The results of SEM and EDX analyses support the strength results obtained by examining the chemical reactions, voids, and elemental ratios within the structure.

These findings indicate the potentially significant advantages of GPC in various applications and suggest that further research could lead to even better results.

Acknowledgements I would like to thank MEDCEM (https://medcem.com.tr) for providing the F-class fly ash used in this study.

Data availability Data will be provided on the request.

References

1. Çelik Aİ, Özbayrak A, Şener A, Acar MC (2022) Effect of activators in different ratios on compressive strength of geopolymer concrete. Can J Civ Eng 50(2):69–79
2. Çelik Aİ, Özkılıç YO (2023) Geopolymer concrete with high strength, workability and setting time using recycled steel wires and basalt powder. Steel Compos Struct 46(5):689–707
3. Çelik Aİ (2023) Mechanical performance of geopolymer concrete based on basalt and marble powder. Iran J Sci Technol Trans Civ Eng 47:2173–2187. https://doi.org/10.1007/s40996-023-01063-4
4. Özkılıç YO, Çelik Aİ, Tunç U, Karalar M, Deifalla A, Alomayri T, Althoey F (2023) The use of crushed recycled glass for alkali activated fly ash based geopolymer concrete and prediction of its capacity. J Mater Res Technol 24:8267–8281
5. Çelik Aİ, Tunç U, Bahrami A, Karalar M, Mydin MAO, Alomayri T, Özkılıç YO (2023) Use of waste glass powder toward more sustainable geopolymer concrete. J Mater Res Technol 24:8533–8546
6. Marvila MT, de Azevedo ARG, de Matos PR, Monteiro SN, Vieira CMF (2021) Materials for production of high and ultra-high performance concrete: review and perspective of possible novel materials. Materials 14(15):4304
7. Alsalman A, Assi LN, Kareem RS, Carter K, Ziehl P (2021) Energy and CO_2 emission assessments of alkali-activated concrete and ordinary Portland cement concrete: a comparative analysis of different grades of concrete. Clean Environ Syst 3:100047
8. Assi L, Carter K, Deaver EE, Anay R, Ziehl P (2018) Sustainable concrete: building a greener future. J Clean Prod 198:1641–1651
9. Li Z, Liu S (2007) Influence of slag as additive on compressive strength of fly ash-based geopolymer. J Mater Civ Eng 19(6):470–474
10. Parthiban K, Saravanarajamohan K, Shobana S, Bhaskar AA (2013) Effect of replacement of slag on the mechanical properties of fly ash based geopolymer concrete. Int J Eng Technol 5(3):2555–2559
11. Rautaray S K, Bera D K, Rath A K (2022) The effects of ground granulated blast-furnace slag blending with fly ash based self compacting Geo-polymer concrete on the workability and strength properties at ambient curing. In: Recent developments in sustainable infrastructure (ICRDSI-2020)—structure and construction management: conference proceedings from ICRDSI-2020, Vol 1. Springer, Singapore, p 567–579
12. Chindaprasirt P, Chareerat T, Sirivivatnanon V (2007) Workability and strength of coarse high calcium fly ash geopolymer. Cement Concr Compos 29(3):224–229
13. Hardjito D, Wallah SE, Sumajouw DM, Rangan BV (2004) On the development of fly ash-based geopolymer concrete. Mater J 101(6):467–472
14. Olivia M, Nikraz H (2012) Properties of fly ash geopolymer concrete designed by taguchi method. Mater Des 1980–2015(36):191–198
15. Mustakim SM, Das SK, Mishra J, Aftab A, Alomayri TS, Assaedi HS, Kaze CR (2021) Improvement in fresh, mechanical and microstructural properties of fly ash-blast furnace slag based geopolymer concrete by addition of nano and micro silica. Silicon 13:2415–2428
16. Prusty JK, Pradhan B (2023) Evaluation of durability and microstructure evolution of chloride added fly ash and fly ash—GGBS based geopolymer concrete. Constr Build Mater 401:132925
17. Tashan J (2022) Flexural behavior evaluation of repaired high strength geopolymer concrete. Compos Struct 300:116144
18. Kalaivani M, Shyamala G, Ramesh S, Angusenthil K, Jagadeesan R (2020) Performance evaluation of fly ash/slag based geopolymer concrete beams with addition of lime. Mater Today Proc 27:652–656
19. Nath SK, Kumar S (2013) Influence of iron making slags on strength and microstructure of fly ash geopolymer. Constr Build Mater 38:924–930
20. Nath P, Sarker PK (2017) Flexural strength and elastic modulus of ambient-cured blended low-calcium fly ash geopolymer concrete. Constr Build Mater 130:22–31
21. Duan P, Yan C, Zhou W (2017) Compressive strength and microstructure of fly ash based geopolymer blended with silica fume under thermal cycle. Cem Concr Compos 78:108–119
22. Tayeh BA, Akeed MH, Qaidi S, Bakar BA (2022) Influence of microsilica and polypropylene fibers on the fresh and mechanical properties of ultra-high performance geopolymer concrete (UHP-GPC). Case Stud Constr Mater 17:e01367
23. Ekinci E, Türkmen İ, Kantarci F, Karakoç MB (2019) The improvement of mechanical, physical and durability characteristics of volcanic tuff based geopolymer concrete by using nano silica, micro silica and styrene—butadiene latex additives at different ratios. Constr Build Mater 201:257–267
24. Yıldızel SA, Özkılıç YO, Bahrami A, Aksoylu C, Başaran B, Hakamy A, Arslan MH (2023) Experimental ınvestigation and analytical prediction of flexural behaviour of reinforced concrete beams with steel fibres extracted from waste tyres. Case Stud Constr Mater 19:e02227. https://doi.org/10.1016/j.cscm.2023.e02227
25. Kumar Mehta P, Paulo JM (2014) Concrete : microstructure, properties, and materials. McGrawHill, New York, p 85–86. ISBN:9780071797870
26. Nataraja MC, Dhang N, Gupta AP (1999) Stress–strain curves for steel–fiber reinforced concrete under compression. Cem Concr Compos 21(5–6):383–390
27. Banthia N, Sappakittipakorn M (2007) Toughness enhancement in steel fiber reinforced concrete through fiber hybridization. Cem Concr Res 37(9):1366–1372
28. Gopalaratnam VS, Gettu R (1995) On the characterization of flexural toughness in fiber reinforced concretes. Cem Concr Compos 17(3):239–254
29. Buratti N, Ferracuti B, Savoia M (2013) Concrete crack reduction in tunnel linings by steel fibre-reinforced concretes. Constr Build Mater 44:249–259
30. Bonakdar A, Babbitt F, Mobasher B (2013) Physical and mechanical characterization of fiber-reinforced aerated concrete (FRAC). Cem Concr Compos 38:82–91
31. Mhaya AM, Huseien GF, Abidin ARZ, Ismail M (2020) Long-term mechanical and durable properties of waste tires rubber crumbs replaced GBFS modified concretes. Constr Build Mater 256:119505
32. Awoyera PO, Akinmusuru JO, Ndambuki JM (2016) Green concrete production with ceramic wastes and laterite. Constr Build Mater 117:29–36
33. Aksoylu C, Özkılıç YO, Hadzima-Nyarko M, Işık E, Arslan MH (2022) Investigation on improvement in shear performance of reinforced-concrete beams produced with recycled steel wires from waste tires. Sustainability 14(20):13360
34. Basaran B, Kalkan I, Aksoylu C, Özkılıç YO, Sabri MMS (2022) Effects of waste powder, fine and coarse marble aggregates on concrete compressive strength. Sustainability 14(21):14388
35. Karalar M, Özkılıç YO, Aksoylu C, Sabri Sabri MM, Beskopylny AN, Stel'makh SA, Shcherban EM (2022) Flexural behavior of reinforced concrete beams using waste marble powder towards application of sustainable concrete. Front Mater 9:1068791

36. Tiwari A, Singh S, Nagar R (2016) Feasibility assessment for partial replacement of fine aggregate to attain cleaner production perspective in concrete: a review. J Clean Prod 135:490–507
37. Al-Fadhli M, Alhumoud J (2017) Properties of concrete containing scrap-tire rubber. J Eng Res Appl 7(3):36–42
38. Eiras JN, Segovia F, Borrachero MV, Monzó J, Bonilla M, Payá J (2014) Physical and mechanical properties of foamed Portland cement composite containing crumb rubber from worn tires. Mater Des 59:550–557
39. Shu X, Huang B (2014) Recycling of waste tire rubber in asphalt and portland cement concrete: an overview. Constr Build Mater 67:217–224
40. Sprince A, Pakrastinsh L, Vatin N (2016) Crack formation in cement-based composites. IOP conf ser: mater sci eng 123:01205
41. Lokuge W, Wilson A, Gunasekara C, Law DW, Setunge S (2018) Design of fly ash geopolymer concrete mix proportions using multivariate adaptive regression spline model. Constr Build Mater 166:472–481
42. Özkılıç YO, Zeybek Ö, Bahrami A, Çelik Aİ, Mydin MAO, Karalar M, Jagadesh P et al (2023) Optimum usage of waste marble powder to reduce use of cement toward eco-friendly concrete. J Mater Res Technol 25:4799–4819
43. ACI Committee 363 (1984) State of the art report on high strength concrete. ACI J Proc 81(4):364–411
44. Standard A (2007) AS 1379:Specification and supply of concrete. Standards Australia, Sydney
45. De Oliveira LB, de Azevedo AR, Marvila MT, Pereira EC, Fediuk R, Vieira CMF (2022) Durability of geopolymers with industrial waste. Case Stud Constr Mater 16:e00839
46. Marvila MT, Azevedo ARGD, Matos PRD, Monteiro SN, Vieira CMF (2021) Rheological and the fresh state properties of alkali-activated mortars by blast furnace slag. Materials 14(8):2069
47. Aydın S, Baradan B (2013) The effect of fiber properties on high performance alkali-activated slag/silica fume mortars. Compos B Eng 45(1):63–69
48. Yoo DY, Kim S, Park GJ, Park JJ, Kim SW (2017) Effects of fiber shape, aspect ratio, and volume fraction on flexural behavior of ultra-high-performance fiber-reinforced cement composites. Compos Struct 174:375–388
49. Ahmed HU, Mohammed AS, Faraj RH, Qaidi SM, Mohammed AA (2022) Compressive strength of geopolymer concrete modified with nano-silica: experimental and modeling investigations. Case Stud Constr Mater 16:e01036
50. Ahmed SN et al (2022) Thermal conductivity and hardened behavior of eco-friendly concrete incorporating waste polypropylene as fine aggregate. Mater Today Proc 57:818–823
51. Ahmed SN, Sor NH, Ahmed MA, Qaidi SM (2022) Thermal conductivity and hardened behavior of eco-friendly concrete incorporating waste polypropylene as fine aggregate. Mater Today Proc 57:818–823
52. Ahmad W, Ahmad A, Ostrowski KA, Aslam F, Joyklad P (2021) A scientometric review of waste material utilization in concrete for sustainable construction. Case Stud Constr Mater 15:e00683. https://doi.org/10.1016/j.cscm.2021.e00683
53. Ahmad J, Aslam F, Martinez-Garcia R, de-Prado-Gil J, Qaidi S, Brahmia A, (2021) Effects of waste glass and waste marble on mechanical and durability performance of concrete. Sci Rep 11:21525. https://doi.org/10.1038/s41598-021-00994-0
54. Wetzel A, Middendorf B (2019) Influence of silica fume on properties of fresh and hardened ultra-high performance concrete based on alkali-activated slag. Cement Concr Compos 100:53–59. https://doi.org/10.1016/j.cemconcomp.2019.03.023
55. Laxmi G, Patil S, Hossiney N, Thejas HK (2023) Effect of hooked end steel fibers on strength and durability properties of ambient cured geopolymer concrete. Case Stud Constr Mater 18:e02122
56. Soni A, Patel J, Poojalakshmi ES, Gupta N, Gupta N, Thomas BS, Ramaswamy KP (2023) Study for the development of flyash and GGBS-based alkali activated foam concrete. Mater Today: Proc. https://doi.org/10.1016/j.matpr.2023.04.581. (Article In Press, Corrected Proof, Available online 12 April 2024)
57. Zhang N, Hedayat A, Han S, Ma S, Sosa HGB, Bernal RPH, Loza RSC (2022) Fracture properties of tailings-based geopolymer incorporated with class F fly ash under mode I loading conditions. Eng Fract Mech 271:108646
58. Reed M, Lokuge W, Karunasena W (2014) Fibre-reinforced geopolymer concrete with ambient curing for in situ applications. J Mater Sci 49:4297–4304
59. Yoo DY, Banthia N (2016) Mechanical properties of ultra-high-performance fiber-reinforced concrete: a review. Cem Concr Compos 73:267–280
60. Zhou Y, Huang J, Yang X, Dong Y, Feng T, Liu J (2021) Enhancing the PVA fiber-matrix interface properties in ultra high performance concrete: an experimental and molecular dynamics study. Constr Build Mater 285:122862
61. Khan MZN, Hao Y, Hao H, Shaikh FUA, Liu K (2018) Mechanical properties of ambient cured high-strength plain and hybrid fiber reinforced geopolymer composites from triaxial compressive tests. Constr Build Mater 185:338–353
62. Wu Z, Shi C, He W, Wu L (2016) Effects of steel fiber content and shape on mechanical properties of ultra high performance concrete. Constr Build Mater 103:8–14
63. Wu Z, Shi C, Khayat KH (2019) Investigation of mechanical properties and shrinkage of ultra-high performance concrete: influence of steel fiber content and shape. Compos B Eng 174:107021
64. Nodehi M, Nodehi SE (2022) Ultra high performance concrete (UHPC): reactive powder concrete, slurry infiltrated fiber concrete and superabsorbent polymer concrete. Innov Infrastruct Solut 7(1):39
65. ASTM (2019) D6400-19: standard specification for labeling of plastics designed to be aerobically composted in municipal or industrial facilities. American Society for Testing and Materials, West Conshohocken. https://www.astm.org
66. Aliabdo AA, Abd Elmoaty M, Salem HA (2016) Effect of water addition, plasticizer and alkaline solution constitution on fly ash based geopolymer concrete performance. Constr Build Mater 121:694–703
67. Rao AK, Kumar DR (2020) Effect of various alkaline binder ratio on geopolymer concrete under ambient curing condition. Mater Today Proc 27:1768–1773
68. Özbayrak A, Kucukgoncu H, Aslanbay HH, Aslanbay YG, Atas O (2023) Comprehensive experimental analysis of the effects of elevated temperatures in geopolymer concretes with variable alkali activator ratios. J Build Eng 68:106108
69. Alghannam M, Albidah A, Abbas H, Al-Salloum Y (2021) Influence of critical parameters of mix proportions on properties of MK-based geopolymer concrete. Arab J Sci Eng 46:4399–4408
70. Mendes BC, Pedroti LG, Vieira CMF, Marvila M, Azevedo AR, de Carvalho JMF, Ribeiro JCL (2021) Application of eco-friendly alternative activators in alkali-activated materials: a review. J Build Eng 35:102010
71. ASTM C143/C143M-15 (2015) Standard test method for slump of hydraulic-cement concrete. ASTM, West Conshohocken, PA, USA, 2015. Available online: https://www.astm.org/DATABASE.CART/HISTORICAL/C143C143M-15A.htm. Accessed 27 Aug 2023
72. ASTM C293/C293M-16 (2021) Standard test method for flexural strength of concrete (Using simple beam with center-point loading). ASTM, West Conshohocken, PA, USA, 2021.

Available online: https://www.astm.org/Standards/C293.htm. Accessed 27 Aug 2023
73. ASTM C476-23 (2023) Standard specification for grout for masonry, West Conshohocken, PA, USA, 2023. Available online: https://www.astm.org/c0476-23.html. Accessed 27 Aug 2023
74. Shang J, Dai JG, Zhao TJ, Guo SY, Zhang P, Mu B (2018) Alternation of traditional cement mortars using fly ash-based geopolymer mortars modified by slag. J Clean Prod 203:746–756
75. Kumar S, Kumar R, Mehrotra SP (2010) Influence of granulated blast furnace slag on the reaction, structure and properties of fly ash based geopolymer. J Mater Sci 45:607–615
76. Lee NK, Kim HK, Park IS, Lee HK (2013) Alkali-activated, cementless, controlled low-strength materials (CLSM) utilizing industrial by-products. Constr Build Mater 49:738–746
77. Farouk Ghazy M (2020) Optimization of recycled concrete aggregate geopolymer bricks by taguchi method. Revista de la Construcción 19(2):244–254
78. Neupane K, Chalmers D, Kidd P (2018) High-strength geopolymer concrete—properties, advantages and challenges. Adv Mater 7(2):15–25
79. Kanagaraj B, Anand N, Alengaram UJ, Praveen B, Tattukolla K (2022) Performance evaluation on engineering properties and sustainability analysis of high strength geopolymer concrete. J Build Eng 60:105147
80. Nodehi M, Aguayo F (2021) Ultra high performance and high strength geopolymer concrete. J Build Pathol Rehabil 6(1):34
81. Dong M, Elchalakani M, Karrech A (2020) Development of high strength one-part geopolymer mortar using sodium metasilicate. Constr Build Mater 236:117611
82. Yierlapalli NK, Boda DK, Patiswara SBL (2023) Effect of ambient curing periods on the mechanical properties of geopolymer concrete prepared with three mineral admixtures and glass fibers. Proc, Mater Today. https://doi.org/10.1016/j.matpr.2023.07.213. (In Press, Corrected Proof, Available online 12 April 2024)
83. Ganesan N, Abraham R, Raj SD (2015) Durability characteristics of steel fibre reinforced geopolymer concrete. Constr Build Mater 93:471–476
84. Bhutta A, Borges PH, Zanotti C, Farooq M, Banthia N (2017) Flexural behavior of geopolymer composites reinforced with steel and polypropylene macro fibers. Cem Concr Compos 80:31–40
85. Farida F M, Hardjasaputra H, Surahman A, Sofwan A, Mukti R R (2023) The effect of polypropylene fiber on the mechanical properties between hybrid fiber geopolymer concrete and geopolymer concrete in elevated temperature. In: IOP conference series: earth and environmental science, vol 1195, IOP Publishing, p 012028
86. Chen C, Zhang X, Hao H (2023) Dynamic tensile properties of geopolymer concrete and fibre reinforced geopolymer concrete. Constr Build Mater 393:132159
87. Hao Y, Hao H (2016) Mechanical properties and behaviour of concrete reinforced with spiral-shaped steel fibres under dynamic splitting tension. Mag Concr Res 68(21):1110–1121
88. Feng KN, Ruan D, Pan Z, Collins F, Bai Y, Wang CM, Duan WH (2014) Effect of strain rate on splitting tensile strength of geopolymer concrete. Mag Concr Res 66(16):825–835
89. Abrishambaf A, Barros JA, Cunha VM (2013) Relation between fibre distribution and post-cracking behaviour in steel fibre reinforced self-compacting concrete panels. Cem Concr Res 51:57–66
90. Chouksey A, Verma M, Dev N, Rahman I, Upreti K (2022) An investigation on the effect of curing conditions on the mechanical and microstructural properties of the geopolymer concrete. Mater Res Express 9(5):055003
91. Fan F, Liu Z, Xu G, Peng H, Cai CS (2018) Mechanical and thermal properties of fly ash based geopolymers. Constr Build Mater 160:66–81
92. Nath P, Sarker PK (2014) Effect of GGBFS on setting, workability and early strength properties of fly ash geopolymer concrete cured in ambient condition. Constr Build Mater 66:163–171
93. García-Lodeiro I, Palomo A, Fernández-Jiménez A, Macphee DE (2011) Compatibility studies between NASH and CASH gels. Study in the ternary diagram Na2O–CaO–Al2O3–SiO2–H2O. Cem Concr Res 41(9):923–931
94. Mehta A, Siddique R (2018) Sustainable geopolymer concrete using ground granulated blast furnace slag and rice husk ash: strength and permeability properties. J Clean Prod 205:49–57

Springer Nature or its licensor (e.g. a society or other partner) holds exclusive rights to this article under a publishing agreement with the author(s) or other rightsholder(s); author self-archiving of the accepted manuscript version of this article is solely governed by the terms of such publishing agreement and applicable law.